Base-free synthesis of benchtop stable Ru(III)-NHC complexes from $RuCl_3 \cdot 3H_2O$ and their use as precursors for Ru(II)-NHC complexes

Nida Shahid, Rahul Kumar Singh, Navdeep Srivastava, Amrendra K. Singh*

A series of Ru(III)-NHC complexes, identified as $[Ru^{III}(PyNHC^{R})(Cl)_3(H_2O)]$ (**1a-c**), have been prepared, starting from $RuCl_3 \cdot 3H_2O$ following a base-free route. The Lewis acidic Ru(III) centre operates via a halide-assisted, electrophilic C-H activation for carbene generation. Best results were obtained with azolium salts having I^- anion while ligand precursors with Cl^-, BF_4^-, and PF_6^- gave no complex formation and those with Br^- gave a product with mixed halides. The structurally simple, air and moisture-stable complexes represent rare examples of paramagnetic Ru(III)-NHC complexes. Further, these benchtop stable Ru(III)-NHC complexes were shown to be excellent metal precursors for the synthesis of new $[Ru^{II}(PyNHC^{R})(Cl)_2(PPh_3)_2]$ (**2a-c**) and $[Ru^{II}(PyNHC^{R})(CNC^{Me})I]PF_6$ (**3a-c**) complexes. All the complexes have been characterised using spectroscopic methods, and structures of **1a**, **1b**, **2c** and **3a** have been determined using the single-crystal X-ray diffraction technique. This work allows easy access to new Ru-NHC complexes for the study of new properties and novel applications.

Introduction

Ru complexes with NHC ligands have become increasingly popular in recent years due to improved catalytic efficiency[1–4] and tuneable stereoelectronic properties,[5–7] which help in catalyst designing.[8] These Ru-NHC complexes have found applications from homogeneous catalysis[9–15] to therapeutic drugs,[16,17] olefin metathesis reactions[18–20] and solar cells (DSSCs).[21–23] In general, the synthesis of Ru-NHC complexes involves one of the common Ru metal precursors $Ru(Cl)_2(PPh_3)_3$,[24] $[Ru(Cl)_2(p\text{-cymene})]_2$,[25] $[Ru(Cl)_2(CO)_2]_n$,[26] $Ru^{II}(Cl)_2(DMSO)_4$,[27] $[Ru(Cl)_2(COD)]_n$,[28] etc., where one or more of the ligands are replaced with the *in situ* generated NHC ligands. Ru-precursor complexes play a significant role in the development of new Ru-complexes. Depending on the design of Ru based catalyst, selection of suitable Ru precursor is the most critical step.[29] Generally, the synthesis of Ru-NHC complexes requires a base for the generation of NHCs from their azolium ligand precursors.[30–32] Involvement of base in such reactions has its shortcomings, namely, the limited or no use of aerobic conditions, less scope to employ green solvents, and possibility of forming undesired side products.[33] Nolan and coworkers have recently developed a "weak base" route[25,33–35] for generating NHC-metal complexes. The simple "weak base" route has been described as a cost-effective and environmentally benign approach which can be extended further with various metals for NHC-based complexes.[23] Among the various synthetic routes reported for the generation of NHCs and their corresponding metal complexes, namely, base-assisted deprotonation of azolium salts followed by metalation, transmetallation of preformed Ag(I)/Cu(I) carbenes, and C-H activation of azolium salts in the presence of metal precursors, C-H activation is considered as one of the simplest routes for the generation of carbene due to the less probability of formation of side product.[36,37]

We have recently started the investigation of Ru(II)-CNC (CNC = pyridine-dicarbene pincer ligands) complexes with smaller N-alkyl wingtips on carbenes for transfer hydrogenation and related catalysis,[38–40] and compared their activity with the molecular catalysts with similar catalyst design.[7] During our investigation, we noticed that even after a few decades of

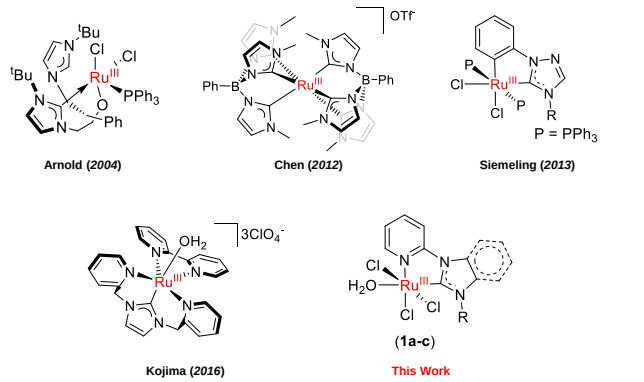

Figure 1. Ru(III)-NHC complexes known so far and complexes (**1a**–**c**) reported in this paper.

[a] *Department of Chemistry, Indian Institute of Technology Indore, Indore 453552, India. Email: aks@iiti.ac.in.*

† Footnotes relating to the title and/or authors should appear here.

Electronic Supplementary Information (ESI) available: [details of any supplementary information available should be included here]. See DOI: 10.1039/x0xx00000x

research in this field, a suitable Ru complex with an NHC ligand, which can be used as a precursor for the synthesis of new complexes with other co-ligands, is still unavailable. Further, it is surprising to note that till now, only four examples of Ru(III)-NHC complexes[41–44] have been reported (Fig. 1.), all of which were obtained upon oxidation of their Ru(II)-NHC analogues.

Herein, we report a "base-free" synthesis of a series of Ru(III)-NHC complexes $[Ru^{III}(PyNHC^{R})(Cl)_3(H_2O)]$ (**1a-c**) {$PyNHC^{R}$ = 3-methyl-1-(pyridine-2-yl)imidazol-2-ylidene (**1a**), 3-isopropyl-1-(pyridine-2-yl)imidazol-2-ylidene (**1b**) and 3-methyl-1-(pyridine-2-yl)benzimidazol-2-ylidene (**1c**)} derived from pyridine functionalised N-alkylated azolium salts, and $RuCl_3{\cdot}3H_2O$. Further, we have utilised these Ru(III)-PyNHC complexes as metal precursors for the synthesis of a series of the corresponding Ru(II)-PyNHC-(PPh_3) complexes (**2a-c**) and Ru(II)-PyNHC-CNC^{Me} ($CNC^{Me}{\cdot}2HBr$ = 2,6-Bis[3-(methyl)imidazolium] pyridine dibromide)pincer complexes (**3a-c**).

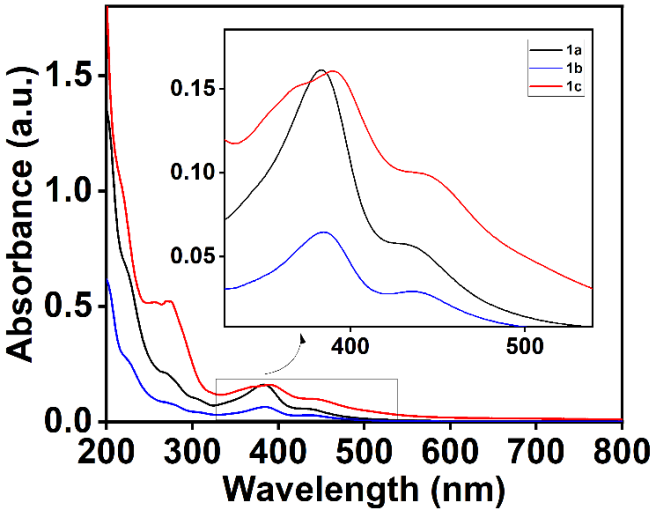

Figure. 2. Plot of UV-vis spectra of complexes **1a-c** in CH_3CN at room temperature. Inset showing the MLCT band of all complexes expected for Ru-$C_{carbene}$ bond.

Results and Discussion

Synthesis and characterisation of 1a-c

The reaction of ligand precursors with $RuCl_3{\cdot}3H_2O$ in a 1:1 ratio in THF at reflux temperature afforded the new Ru(III)-PyNHC complexes **1a-c** (Scheme 1) depending on the counterion of the azolium salt. Initial attempts with azolium salts having BF_4^- or PF_6^- counterions (to prevent the formation of mixed-halide complexes) gave no reaction with or without a base. In the presence of weak or strong bases, such as NEt_3, K_2CO_3, KOH, and KO^tBu, a black powder was obtained, which is insoluble in water or any organic solvent. The first successful preparation of **1a** and **1c** was achieved with the ligand precursor having iodide counterions. No chemical additive, like a base, was required for the reaction, and no indication of mixed-halide products was observed in the preparation of **1a** and **1c** (via mass spectrometry of crude product). Similarly, for **1b**, the azolium salt with bromide ions resulted in the desired product; however, in this case, mixed halide complexes were observed in the LC-MS of the crude product. Surprisingly, the corresponding azolium salt with chloride anions did not give product **1b** under the same conditions. Switching over to the ligand precursor with iodide counterion improved the yield for **1b,** and, again, the LC-MS of crude product indicated no formation of mixed-halide complexes.

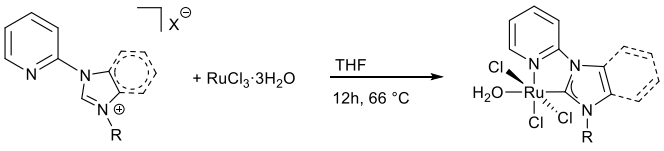

$PyIm^{R}{\cdot}HX$, $PyBIm^{R}{\cdot}HX$
R = Me; X = I
R = iPr; X = I; clean reaction
R = iPr; X = Br; mixed-halide product
R = iPr; X = Cl, BF_4, PF_6; no reaction

	$PyIm^{R}$	$PyBIm^{R}$
R = Me;	**1a**	**1c**
R = iPr;	**1b**	--

Scheme 1. Synthesis of Ru(III)-PyNHC complexes (**1a-c**).

It is reasonable to believe that the Lewis acidic Ru(III) metal centre operates via a halide-assisted electrophilic C-H activation for the generation of carbene, where the C-H activation is also affected by the halide ions of the azolium ion pairs. The synthesis of **1a-c** has been scaled up to the gram scale starting from 1 g of $RuCl_3{\cdot}3H_2O$. All three complexes were obtained in excellent yields (75–82%) from iodide salts of their corresponding azolium precursors.

Complexes **1a-c** have been characterised by IR, UV-Vis spectroscopy, and ESI^+ mass spectrometry. The paramagnetic nature (low spin d^5) of the Ru centre in these complexes was confirmed by measurement of their magnetic moment using the Evans method.[45] The values for magnetic moments were found within the range of 1.70–1.72 BM establishing the presence of one unpaired electron. To determine the thermal stability of complexes **1a-c**, thermogravimetric analysis was performed under a nitrogen atmosphere. The plots showed no weight loss in complexes up to 150 °C. The loss of H_2O molecule from complexes was observed at 250 °C (**1a**), 230 °C (**1b**), and 175 °C (**1c**), and the gradual decrease in weight can be attributed to the loss of chloride ligands present in the system. Stretching frequencies for C=N and C-C bonds obtained using IR spectroscopy were compared with the ligand precursors and found to lie within the expected range 1500-1200 cm^{-1} ($Im_{C=N}$), and 1600-1400 cm^{-1} (Py_{C-C}) and C-H stretch lie in a range 3100-3000 cm^{-1}.The characteristic MLCT absorption maxima in UV-vis spectra for the Ru-NHC bond in the three complexes were observed at 384 nm (5337 $M^{-1}cm^{-1}$) (**1a**), 385 nm (3181 $M^{-1}cm^{-1}$) (**1b**) and 392 nm (5132 $M^{-1}cm^{-1}$) (**1c**) (Fig.3.). ESI^+-MS spectrograms showed peaks for the fragments $[M\text{-}Cl]^+$, $[M\text{-}Cl\text{-}H_2O]^+$, and $[M\text{-}Cl\text{-}H_2O\text{+}S]^+$ (where S=Solvent, i.e., MeCN or MeOH), in complexes **1a-c**. HRMS spectrogram of the molecular ion peak at m/z assignable to $[M\text{-}Cl]^+$, i.e., 348.9315 (**1a**), 376.9613 (**1b**), and 398.9501 (**1c**) confirmed the elemental

composition (See SI). Complexes **1a** and **1b** have also been characterised by Powder XRD, and their structures have been determined by the single-crystal X-ray diffraction technique.

Description of crystal structures of 1a-b

Molecular structures of **1a** and **1b** were determined using the single-crystal X-ray diffraction technique. Complexes **1a** and **1b** crystallised in orthorhombic (*Pna2₁*) and monoclinic (*I2/a*) crystal systems, respectively. The structures exhibited a pseudo-octahedral geometry around the Ru(III) centre. The bidentate ligand forms a five-membered metallacycle with a bite angle of 79.7(7)° and 78.34(19)° in **1a** and **1b,** respectively. In both the structures, the coordinated H_2O ligand was replaced by the solvent of crystallisation, i.e., MeCN in **1a** (Fig. 3) and MeOH in **1b** (Fig. 4). Therefore, the structure obtained for complex **1a** is denoted as **1a-MeCN**, and that of **1b** is denoted as **1b-MeOH**. Acetonitrile was observed trans to pyridine N-atom in **1a-MeCN,** whereas in **1b-MeOH**, π-donor methanol was found trans to the NHC. In another complex [Ru^{II}(PyNHC$^{t\text{-}Bu}$)(Cl)$_3$(NO)],[46,47] reported earlier, the π-acid ligand NO has also been found trans to the pyridine N-atom. The Ru-$C_{carbene}$ bond distance in **1b-MeOH** (1.972(2)Å) is shorter than the corresponding distance in **1a-MeCN** (1.998(6)Å) and the previously reported Ru(II)-NO (2.049(5) Å).[46] The shortening of bond length in **1b-MeOH** could be due to the increased π-back donation from the Ru(III) centre with a π-donor MeOH ligand at the trans position. Selected bond parameters have been listed in Table S2 (See SI). DFT calculations of isomeric cis/trans-forms w.r.t position of solvent molecule from pyridine N-atom confirms that in the case of π-acid MeCN ligand, isomer with the solvent trans to pyridine was found to be thermodynamically stable while in case of π-donor ligand structure with the solvent molecule trans to NHC was found to be stable.

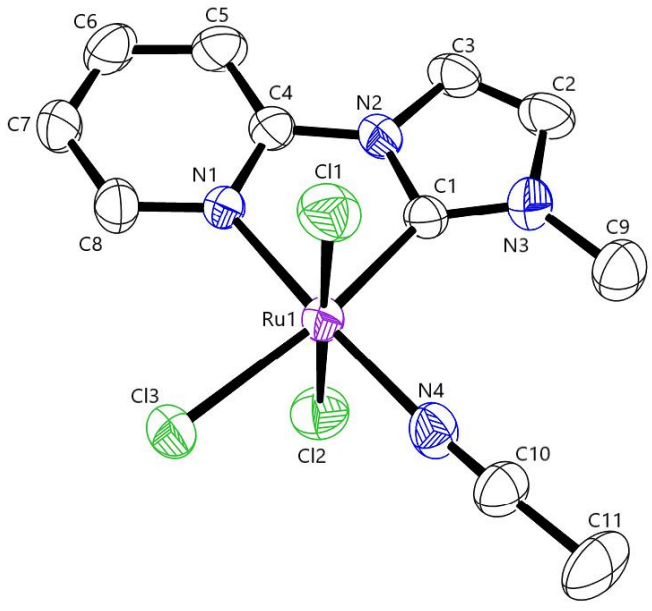

Figure 3. ORTEP diagrams for complex 1a-MeCN obtained from X-ray diffraction. Hydrogen atoms and solvent molecule are excluded for clarity. Ellipsoids are shown at the 50% probability level. Selected bond distances(Å) and bond angles(º) are Ru1-C1 1.998(6); Ru1-N1 2.042(5); Ru1-N4 2.038(6); C1-Ru1-N1 77.9(2); and N1-Ru1-N4 176.6(2).

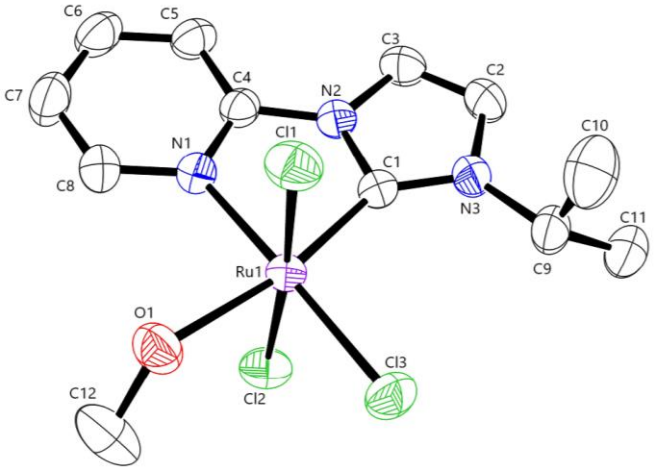

Figure 4. ORTEP diagrams for complex **1b-MeOH** obtained from X-ray diffraction. Hydrogen atoms and solvent molecule are excluded for clarity. Ellipsoids are shown at the 50% probability level. Selected bond distances(Å) and bond angles (°) are Ru1-C1 1.972(2); Ru1-N1 2.073(2); Ru1-O1 2.2259(18); C1-Ru1-N1 78.32(9); and C1-Ru1-O1 169.35(9)

Use of complexes 1a-c as precursors

Complexes **1a-c** represent easily accessible Ru(III)-PyNHC complexes with a well-defined composition compared to $RuCl_3{\cdot}3H_2O$. These complexes were found to be air and moisture stable and can be stored at benchtop for several months with

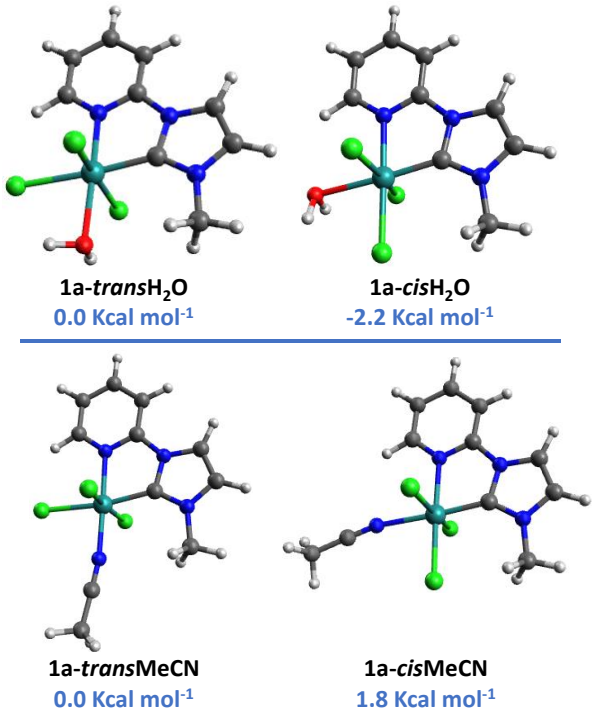

Figure 5. Optimised cis/trans isomeric forms of 1a w.r.t solvent molecule (H2O and MeCN) and relative Gibbs free energies (at 298.15 K) and 1M solution.

no sign of decay. Further, these complexes enrich the list of very rare Ru(III)-NHC complexes,[42–44] which have, so far, been obtained by oxidising a Ru(II)-NHC complex as Ru(II) precursor.[41] To check the usefulness of **1a-c** as starting material for the preparation of Ru(II)-NHC complexes with different ancillary ligands, complexes **1a-c** have been used to prepare the phosphine complexes **2a-c** following the same procedure as preparation of $RuCl_2(PPh_3)_3$ from $RuCl_3{\cdot}3H_2O$. Further, to demonstrate the thermal stability of these complexes as metal precursors, Ru-PyNHC-CNC pincer complexes **3a-c** have been prepared under ethylene glycol reflux conditions (190 °C).

Synthesis of phosphine complexes 2a-c from 1a-c

The reaction of complexes **1a-c** with a 6-fold excess of triphenylphosphine in methanol at reflux temperature gave the corresponding Ru(II)-PyNHC-(PPh_3) complexes formulated as $[Ru^{II}(PyNHC^{R})(Cl)_2(PPh_3)_2]$ **2a-c** in 60–80% yield (Scheme 2). The air-stable, yellow complexes were characterised by ESI^+-MS, ^1H and ^{31}P NMR, and the molecular structure of **2c** was determined by single-crystal X-ray diffraction technique. HRMS spectrogram exhibited a molecular ion peak at m/z fragment 820.1361 (**2a**), 848.1688 (**2b**), and 870.1545 (**2c**) assignable to $[M\text{-}Cl]^+$.

The poor solubility of **2a–c** in common organic solvents and phosphine dissociation in solution makes it difficult to obtain good quality ^1H NMR data. However, for **2b** in CD_3CN and **2c** in DMSO-d_6, ^1H NMR could be obtained with a sufficient S/N ratio for the identification of relevant peaks. Compound **2a** was not soluble in CD_3CN, and PPh_3 dissociation in DMSO-d_6 resulted in poor-quality ^1H NMR data. The ^{31}P NMR spectrum of **2b** in CD_3CN shows a singlet at 25.9 ppm with very small signals for one phosphine-dissociated species at 49.3 ppm and the free PPh_3 at -6 ppm. The corresponding signals for complex **2a** were observed at 26.7 ppm and 35.4 ppm and for **2c** at 24.2 ppm, and 33.3 ppm, respectively, with significant PPh_3 dissociation.

Description of crystal structure 2c

The structure of complex **2c** has been determined by X-ray crystallography (Fig. 6). It crystallised in a monoclinic ($P2_1/c$) space group and displayed a pseudo-octahedral geometry around the Ru(II) centre with a solvent (MeCN) bound to the metal and a Cl^- counterion in the lattice (hence denoted as **2c-MeCN**.The Ru1-C1 bond length in **2c-MeCN** is 1.964(4) Å, whereas in Ru(III)-PyNHC analogues, the values for these bond distances in **1a-MeCN** and **1b-MeOH** are 2.052(16) Å and 2.007(5) Å respectively. The short Ru-$C_{carbene}$ bond in **2c- MeCN** can be attributed to the increased π-back-donation from the Ru(II) compared to Ru(III) metal centre. In an example reported by Siemeling et al.,[41] the lengthening of bond distance was also observed upon oxidation from Ru(II)-NHC (1.972(2) Å) to Ru(III)-NHC (2.032(8) Å). Other relevant bond parameters are listed in Table S2 (See SI).

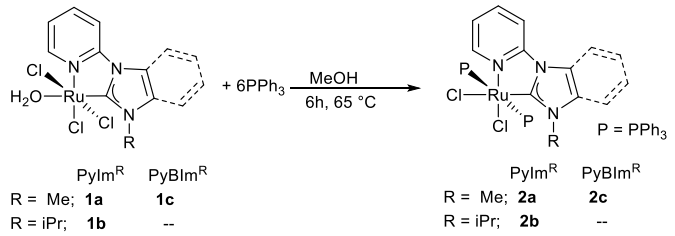

Scheme 3. Synthesis of Ru(II)-PyNHC-PPh3 (2a-c) from Ru(III)-PyNHC complexes (1a-c).

Synthesis of CNC-pincer complexes 3a-c from 1a-c

In another example for the preparation of derivatives of **1a–c**, we have synthesised a series of $[Ru^{II}(PyNHC^{R})(CNC^{Me})I]PF_6$ pincer complexes **3a-c** starting from **1a-c** (Scheme 3). This approach involves the reaction of CNC pincer ligand precursor with our precursor complexes **1a-c** in ethylene glycol at reflux temperature (190 °C) to yield complexes **3a-c**. A complex, $[Ru^{II}(PyNHC^{n\text{-}Bu})(CNC^{n\text{-}Bu})Br]PF_6$, structurally similar to **3a-c** has been reported in the literature,[48] where the synthetic strategy involves the preparation of Ru-$CNC^{n\text{-}Bu}$ pincer complex from $[Ru(COD)Cl_2]_x$ polymer followed by reaction with $PyNHC^{n\text{-}Bu}{\cdot}HBr$ in the presence of Ag_2O as a base.

The successful synthesis of **3a-c** indicates the thermal stability of Ru(III)-PyNHC precursors **1a-c**. NaI was added to reduce the possibility of mixed halide complexes. Complexes **3a-c** were characterised by ESI^+ mass spectrometry and NMR spectroscopy. HR-MS spectrogram exhibited a molecular ion

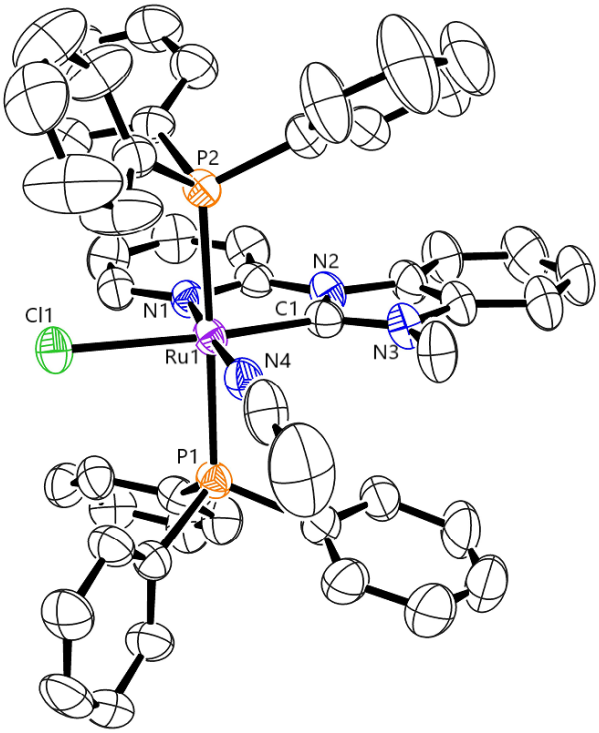

Figure 6. ORTEP diagram of complex **2c-MeCN** obtained from X-ray diffraction. Hydrogen atoms and one Cl- anion present in the lattice are excluded for clarity. Ellipsoids are shown at the 50% probability level. Selected bond distances(Å) and bond angles (°) are Ru1-C1 1.964(4); Ru1-P1 2.3978(12); Ru1-P2 2.4290(12); Ru1-Cl1 2.5005(12); Ru-N1 2.088(4); Ru1-N4 2.067(4); P1- Ru1-P2 178.08(4); C1-Ru1-N1 78.99(17); and N1-Ru1-N4 175.72(14)

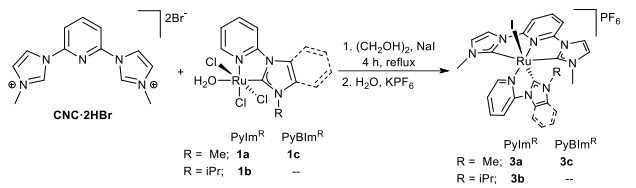

Scheme 3. Synthesis of Ru(II)-PyNHC-CNCMe pincer complexes (3a-c) from Ru(III)-PyNHC complexes (1a-c)

peak at m/z fragment 627.0079 (**3a**), 655.0365 (**3b**), and 677.0242 (**3c**) assignable to $[M\text{-}PF_6]^+$. The ^1H and ^{13}C NMR spectra of complexes **3a-c** in DMSO-d_6 show two distinct sets of signals, indicating the existence of two isomeric structures. In ^1H NMR, in addition to the expected, downfield shifted signal (d, 10.27 (**3a**), 10.29 (**3b**), and 10.44 ppm (**3c**) doublet) for the proton at the ortho position of the pyridine unit in the bidentate ligand PyNHC^R (similar to the reported complex [Ru^{II}(PyNHC$^{n\text{-}Bu}$)(CNC$^{n\text{-}Bu}$)Br]PF_6), another doublet at δ 9.81 (**3a**), 9.81 (**3b**) and 9.90 ppm (**3c**) are also obtained. Similarly, in the alkyl region, two sets of peaks, double the number of expected signals, are obtained. This could be due to cis/trans-isomers with respect to the two pyridine units, as has been reported earlier for structurally similar Ru-tpy complexes (tpy = terpyridine).[49] Another possibility for the existence of two signals could arise due to iodide substitution by a dmso-d_6 molecule resulting in an equilibrium between iodide coordinated and dissociated forms. Therefore, the trans-isomer or the iodide coordinated form show a downfield shifted signal, but the cis-isomer or the iodide dissociated form do not show such a shift. The ^{13}C NMR spectra also show two sets of peaks for the two types of carbene for CNC^{Me} ligand and the bidentate (PyNHC^R) ligand. The exact reason, out of the two possibilities, for the existence of two sets of peaks, is uncertain at this time and is currently being investigated.

The solid-state structure and geometry around the Ru centre in **3a** have been confirmed by the single-crystal X-ray diffraction technique. It crystallised in a monoclinic ($P2_1/c$) space group, and the structure revealed the three five-membered metallacycles, two of which are formed by pincer ligand, and one is due to the bidentate ligand framework. The crystal structure of **3a** shows an octahedral geometry around the Ru(II) centre and confirms the structure as depicted in Scheme 3; however, due to poor diffraction, the data quality is not sufficient to discuss bond parameters.

Conclusions

In summary, we report a base-free, scalable synthesis of a series of new, benchtop stable Ru(III)-NHC complexes **1a**-**c** based on a bidentate PyNHC^R ligand framework bearing R = Me, and ^{i}Pr alkyl wingtips. alkyl wingtips. These Ru(III) complexes serve as metal precursors for the preparation of phosphine complexes, **2a**-**c** and CNC pincer complexes **3a-c**. The synthesis of complexes **3a-c** indicates the thermal stability as well as the usability of complexes **1a-c** in harsh reaction conditions. All new compounds have been characterised by usual characterisation techniques, and the structures of **1a**, **1b**, **2c**, and **3a** have been confirmed by single-crystal X-ray diffraction technique. The results reported here present a straightforward route to prepare Ru(III)-NHC complexes from simple starting materials. Further studies on the synthesis of analogues Ru(III)-NHC complexes with different alkyl wingtips of the NHC units, variation of azole rings and their use as metal precursors for the synthesis of Ru(II)-NHC complexes with different ligands are currently undergoing.

Experimental Section

Materials

All reactions were performed in oven dried glassware under an inert atmosphere using Schlenk line technique. Azoles (1-H-imidazole and 1-H-benzimidazole) were purchased from Sisco Research Laboratories Pvt. Ltd. (SRL)-India. Solvents: dichloromethane (DCM), hexane, ethyl acetate (EtOAc), tetrahydrofuran (THF), methanol (MeOH), and ethylene glycol $(CH_2OH)_2$ were purchased from S. D. Fine-Chem Limited and used after purification. Methanol has been degassed before using as a solvent in a reaction. Deuterated NMR solvents, DMSO-d_6 and CD_3CN, were purchased from Eurisotop and Sisco Research Laboratories Pvt. Ltd. (SRL) respectively and distilled from CaH_2 before use. 2-Bromopyridine was purchased from Spectrochem (India). Alkyl halides and $RuCl_3{\cdot}3H_2O$ were purchased from Spectrochem (India) and Sigma-Aldrich respectively.

Characterisation methods

ESI$^+$-MS chromatograms were recorded using Bruker-Daltonics-MicroTOF-QII mass spectrometer for exact mass and true isotopic measurement. Electronic absorption spectra were recorded in a quartz cuvette using a Varian UV-vis spectrophotometer. A Bruker Avance (III) spectrometer operating at 400 MHz (^1H), 162 MHz (^{31}P), and 100 MHz (^{13}C) and Bruker Avance NEO spectrometer operating at 500 MHz (^1H), 202 (^{31}P), and 126 MHz (^{13}C) were used to record the NMR spectra. Magnetic susceptibilities (χ) were evaluated using NMR Evans method[45] by taking the chemical shift difference in residual solvent peak DMF, in the mixture of DMF:DMSO-d_6 :: 2:3 in 0.5 ml, in ^1H NMR spectra, recorded at 400 MHz spectrometer at room temperature, which was further used to calculate magnetic moment (μ_B). The mixture of solvents was taken to suppress the coordination of DMSO-d_6 to Ru(III) centre. Powder XRD patterns were recorded on Rigaku SmartLab X-ray diffractometer using Cu-Kα radiation. Thermogravimetric analyses were carried out on a TGA-50 series thermal analyser within the temperature range from 25 to 800 ºC under inert atmosphere. ATR (attenuated total reflectance) spectra were recorded using Bruker Alpha II spectrophotometer in solid state in the wavenumber range 4000-500 cm^{-1}. Elemental analyses were carried out on The Thermo Scientific FLASH 2000 (formerly the FLASH EA1112) CHNS-O elemental analyser.

X-ray data collection and refinement

The single crystal X-ray diffraction data of complexes were obtained using dual-core Agilent technologies (Oxford Diffraction) Super Nova CCD System equipped with micro focus Mo and Cu sources. Data was recorded at 293(2) K using graphite-mono chromated Mo Kα radiation source (λ_α = 0.71073 Å) for complexes **1b** and **2c**, and Cu Kα radiation source (λ_α = 1.54184) for complexes **1a** and **3a**. Data were collected using CrysAlisPro CCD and reduced using CrysAlisPro RED software. The SHELXT program[50] was used to solve the structure with intrinsic phasing, and refinement by the full matrix least-squares on F^2 was carried out using SHELXL[50] within Olex2 program[51] for graphical interface. For **2c**, a solvent mask was calculated, and 168 electrons were found in a volume of 1262 Å^3 in one void per unit cell. This is consistent with the presence of 2[CH_3CN] per asymmetric unit which account for 176 electrons per unit cell. All non-hydrogen atoms were refined anisotropically. ORTEP-3[52] was used to create the images. All crystallographic and bond parameters of complexes **1a**, **1b**, **2c**, and **3a** are provided in Table S1–S2. CCDC 2177433-2177436 contain supplementary crystallographic data of this paper.

DFT calculations

All DFT calculations were performed using the ORCA 5.0.3 program package developed by Neese and coworkers.[53,54] The geometry optimisations and frequency calculations in gaseous phase were carried out starting from X-ray geometry using M06L[55] meta-generalised gradient approximation (m-GGA) functional along with "DEFGRID3" integration grids and Ahlrichs's def2-TZVP with def2-ECP on Ru, and def2-SVP basis set on all other atoms (BS1).[56] Stationary points were confirmed to have no imaginary frequency. Thermochemical properties were calculated at T=298.15 K. Single point calculations were performed for solvation in "water", "acetonitrile" and "tetrahydrofuran" according to SMD model at the same level of theory as the geometry optimisations to obtain the solvation energies in these solvents.[57] Grimme's geometrical counterpoise correction (gCP)[58] was applied for all calculations during geometry optimisation, frequency calculations and single point energy calculations using SMD solvation model. For final energy, single-point calculations were performed using a hybrid GGA functional PBE0[59] and a larger basis set def2-QZVPP and def2-ECP on Ru, and def2-TZVPP on all other atoms (BS2).[60] Dispersion corrections were applied during the final single point energy calculations with PBE0 functional according to Grimme's D4 scheme.[61] Electronic energies obtained from final single point calculations were corrected for solvation energies, total corrections obtained from the thermochemical calculation and standard state conversion from 1 atm to 1M to get the Gibbs free energies in 1M solution. Change in Gibbs free energies, ΔG are reported in Kcal/mol.

Synthesis of ligand precursors

Ligand precursors L^1·HI, L^2·HBr, and L^3·HI were prepared following the synthetic procedure reported in literature.[62–64] To eliminate the possibility for the formation of mixed halide complexes observed in synthesis of **1b** from L^2·HBr, different analogues of ligand L^2·HX (X = Cl, I, BF_4, and PF_6) were prepared accordingly. L^2·HCl was synthesised using 2-Chloropyridine and 1-methyl-1H-imidazole, L^2·HI was prepared by anion exchange of L^2·HBr with NaI in acetone at room temperature, the precipitate of NaBr was crashed out from the solution and filtrate was reduced under rotary evaporator and triturated with hexane to obtain the desired compound in good yield. Similarly, L^2·HBF_4 and L^2·HPF_6 were obtained by ion exchange with $NaBF_4$ and NH_4PF_6 respectively in aqueous medium.

Synthesis of complexes

Synthesis of 1a: Under an inert atmosphere, a 50 ml Schlenk tube was charged with L^1·HI (1.74 mmol, 0.500 g), $RuCl_3 \cdot 3H_2O$ (1.74 mmol, 0.455 g) and THF (7–8 ml). The reaction mixture was stirred for 12 hours at reflux temperature resulting in brown precipitate and a dark brown solution. Subsequently, the brown solid product was filtered and washed several times with THF and dried under vacuum. Yield = 0.591 g (1.54 mmol, 78%). Liquid chromatography mass spectrometry (LCMS) : 330.92 [M-Cl-H_2O]$^+$, 348.93 [M-Cl]$^+$, 366.94 [M-Cl+H_2O]$^+$, 698.81 [2M-Cl-$2H_2O$]$^+$. High resolution mass spectrometry (HRMS) for [M-Cl]$^+$ ($C_9H_{11}Cl_2N_3ORu$) in CH_3CN: Calculated: 348.9313; Found: 348.9315. Magnetic moment, μ_B = 1.72 BM. UV-vis λ_{max}/CH_3CN, nm (ε, M^{-1}, cm^{-1}): 434 (1944), 384 (5337). The X-ray quality crystals were obtained by slow diffusion of diethyl ether in acetonitrile solution of **1a** at 4 °C. Anal. Calcd. for $C_{11}H_{12}Cl_3N_4Ru$ (M = 407.66 g/mol): C 32.41, H 2.97, N 13.74, Found: C 32.03, H 2.94, N 13.39%.

Synthesis of 1b: Following the synthetic procedure described for **1a**, L^2·HBr (1.85 mmol, 500 mg) and $RuCl_3 \cdot 3H_2O$ ((1.85 mmol, 0.485 g) were added in THF (7-8 ml). The reaction mixture was stirred for 12 hours at reflux temperature. The precipitate obtained was filtered and washed several times with THF and dried under vacuum. The product was collected as red brown solid. Yield = 0.226 g (1.017 mmol, 55%). LCMS: 358.96 [M-Cl-H_2O]$^+$, 376.96 [M-Cl]$^+$, 399.97 [M-Cl-H_2O+CH_3CN]$^+$. HRMS for [M-Cl]$^+$ ($C_9H_{11}Cl_3N_3ORu$) in CH_3CN: Calculated: 376.9636; Found: 376.9613. Magnetic moment, μ_B = 1.72 BM. UV-vis λ_{max}/CH_3CN, nm (ε, M^{-1}, cm^{-1}): 432 (3492), 381 (4558). The X-ray quality crystals were obtained by slow diffusion of diethyl ether in methanol solution of **1b** at 4 °C.

1b synthesized from L^2·HI, LCMS (ESI$^+$): 358.96 [M-Cl-H_2O]$^+$, 376.96 [M-Cl]$^+$, 399.97 [M-Cl-H_2O+CH_3CN]$^+$, 754.88 [2M-2Cl]$^+$. HRMS for [M-Cl]$^+$ ($C_{11}H_{15}Cl_2N_3ORu$) in CH_3CN: Calculated: 376.9636; Found: 376.9613. Magnetic moment, μ_B = 1.72 BM. UV-vis λ_{max}/CH_3CN, nm (ε, M^{-1}, cm^{-1}): 432 (3492), 385 (3181). The X-ray quality crystals were obtained by slow diffusion of diethyl ether in methanol solution of **1b** at 4 °C. Attempts at elemental analyses failed to give the acceptable nitrogen content, while carbon and hydrogen are in the acceptable range. We suspect an instrumental error in the N-content determination. Anal. Calcd. for $C_{12}H_{17}Cl_3N_3ORu$ (M = 425.94 g/mol): C 33.78, H 4.02, N 9.85, Found: C 33.53, H 4.38, N 7.44%.

Synthesis of 1c: Following the synthetic procedure described for **1a**, L^3·HI (1.48 mmol, 500 mg) and $RuCl_3·3H_2O$ (1.48 mmol, 0.387 g) were added in THF (7–8 ml). The reaction mixture was stirred for 12 hours at reflux temperature resulting in dark brown solid and dark brown solution. Subsequently, the brown solid product was filtered and washed several times with THF and dried under vacuum. Yield = 0.530 g (1.22 mmol, 82%). LCMS: 377.95 $[M\text{-}2Cl\text{-}H_2O+CH_3OH]^+$, 418.98 $[M\text{-}2Cl\text{-}H_2O+CH_3OH+CH_3CN]^+$. HRMS for $[M\text{-}Cl]^+$ ($C_{13}H_{11}Cl_2N_3ORu$) in CH_3CN: Calculated: 398.9471; Found: 398.9501. Magnetic moment, μ_B = 1.73 BM. UV-vis λ_{max}/CH_3CN, nm (ε, M^{-1}, cm^{-1}): 446 (3228), 392 (5132). Attempts at elemental analyses failed to give the acceptable nitrogen content, while carbon and hydrogen are in the acceptable range. We suspect an instrumental error in the N-content determination. Anal. Calcd. for $C_{13}H_{13}Cl_3N_3ORu·1H_2O$ (M = 452.70 g/mol): C 34.49, H 3.34, N 9.28, Found: C 34.75, H 3.10, N 14.6%.

Gram-Scale synthesis of complexes 1a-c: Following the procedure described above, ligand precursors were reacted with $RuCl_3·xH_2O$ (3.82 mmol, 1 g) in a 1:1 ratio in THF at reflux temperature. The products were filtered, washed several times with THF and dried under vacuo. An overall yield obtained, 1.09 g (2.86 mmol, 75%) (**1a**), 1.117 g (2.71 mmol, 71%) (**1b**), and 1.29 g (2.98 mmol, 78%) (**1c**).

Synthesis of 2a: An oven dried Schlenk tube equipped with magnetic stirrer bar was charged with 7 mL bench top methanol and degassed under N_2 atmosphere for 30 min at reflux temperature. The reaction vessel was cooled to room temperature under inert atmosphere and added triphenylphosphine (PPh_3) (7.79 mmol, 2.043 g) and **1a** (1.299 mmol, 0.500 g) in an equivalent ratio of 6 to 1 respectively. The reaction was again heated to reflux at 65 °C for 6 hours. After cooling the reaction vessel, the bright yellow solid was collected and washed with methanol and diethyl ether and dried under vacuo. Yield = 0.700 g (0.817 mmol, 63%). M.P. 225 ºC. LCMS: 820.13 $[M\text{-}Cl]^+$, 861.15 $[M\text{-}Cl+CH_3CN]^+$. HRMS for $[M\text{-}Cl]^+$ ($C_{45}H_{39}Cl_2N_3P_2Ru$) in CH_3CN: Calculated: 820.1355; Found: 820.1361. ^{31}P NMR (202 MHz, DMSO): 26.71, 35.39. Anal. Calcd. for $C_{45}H_{39}Cl_2N_3P_2Ru·1CH_3OH$ (M = 887.78 g/mol): C 62.23, H 4.88, N 4.73, Found: C 61.77, H 4.68, N 4.50%.

Synthesis of 2b: Following the synthetic procedure described for **2a**, complex **2b** was prepared from **1b**. The bench top methanol was degassed under N_2 atmosphere and cooled to room temperature and added **1b** (1.211 mmol, 0.500 g) and triphenylphosphine in an equivalent ratio of 1 to 6 respectively. The reaction was again heated to reflux at 65 °C for 6 hours. The pale-yellow solid was collected and washed with methanol and diethyl ether and dried under vacuo. Yield = 0.865g (0.979 mmol, 81%). M.P. 175 ºC. LCMS: 586.07 $[M\text{-}Cl\text{-}PPh_3]^+$, 627.10 $[M\text{-}Cl\text{-}PPh_3+CH_3CN]^+$, 848.17 $[M\text{-}Cl]^+$, 889.18 $[M\text{-}Cl+CH_3CN]^+$. HRMS for $[M\text{-}Cl]^+$ ($C_{47}H_{43}ClN_3P_2Ru$) in CH_3CN: Calculated: 848.1668; Found: 848.1688. UV-vis λ_{max}/CH_3CN, nm (ε, M^{-1}, cm^{-1}): 323 (5983). ^1H NMR (500 MHz, CD_3CN) δ 8.50 (d, *J* = 5.8 Hz, 1H), 7.91 (d, *J* = 2.5 Hz, 1H), 7.57 – 7.52 (m, 1H), 7.50 (dd, *J* = 7.6, 2.8 Hz, 1H), 7.33 (t, *J* = 7.4 Hz, 6H), 7.22 (t, *J* = 7.6 Hz, 12H), 7.19 – 7.14 (m, 12H), 7.09 (d, *J* = 2.2 Hz, 1H), 6.55 (t, *J* = 6.6 Hz, 1H), 4.01 – 3.92 (m, 1H), 0.62 (d, *J* = 6.7 Hz, 6H). ^{31}P NMR (202 MHz, CD_3CN) δ 49.94, 25.88. Attempts at elemental analyses failed to give the acceptable nitrogen content, while carbon and hydrogen are in the acceptable range. We suspect an instrumental error in the N-content determination. Anal. Calcd. for $C_{47}H_{43}Cl_2N_3P_2Ru·2H_2O.1CH_3OH$ (M = 951.87 g/mol): C 60.57, H 5.40, N 4.41, Found: C 60.80, H 5.20, N 5.00%.

Synthesis of 2c: Following the synthetic procedure described for **2a**, complex **2c** was prepared from **1c**. The bench top methanol was degassed under N_2 atmosphere and cooled to room temperature and added **1c** (1.152 mmol, 0.500 g) and triphenylphosphine in an equivalent ratio of 1 to 6 respectively. The reaction was again heated to reflux at 65 °C for 6 hours. The light brown solid was collected and washed with methanol and diethyl ether and dried under vacuo. Yield = 0.907g (1.001 mmol, 87%). M.P. 160 ºC. LCMS: 689.05 $[M\text{-}Cl\text{-}PPh_3]^+$, 870.15 [M-Cl]+, 911.18 $[M\text{-}Cl+CH_3CN]^+$. HRMS for $[M\text{-}Cl]^+$ ($C_{49}H_{41}Cl_2N_3P_2Ru$) in CH_3CN: Calculated: 870.1512; Found: 8701545. UV-vis λ_{max}/CH_3CN, nm (ε, M^{-1}, cm^{-1}): 306 (8145). ^1H NMR (500 MHz, DMSO) δ 9.37 (d, *J* = 5.7 Hz, 1H), 8.97 (d, *J* = 5.9 Hz, 1H), 8.17 (d, *J* = 7.8 Hz, 1H), 8.06 (d, *J* = 8.3 Hz, 1H), 8.02 (d, *J* = 8.4 Hz, 1H), 7.74 (dd, 1H), 7.70 (d, *J* = 7.9 Hz, 1H), 7.25 – 7.18 (m, 12H), 7.02 (td, *J* = 7.9, 2.1 Hz, 6H), 6.97 (t, *J* = 7.5, 6.8 Hz, 12H), 6.38 (t, *J* = 6.6 Hz, 1H), 3.71 (s, 3H). ^{31}P NMR (202 MHz, DMSO) δ 33.28, 24.22. The X-ray quality crystals were obtained by slow diffusion of diethyl ether in acetonitrile solution of **2c** at -18 °C. Attempts at elemental analyses failed to give the acceptable nitrogen content, while carbon and hydrogen are in the acceptable range. We suspect an instrumental error in the N-content determination. Anal. Calcd. for $C_{49}H_{41}Cl_2N_3P_2Ru·1CH_3OH$ (M = 937.84 g/mol): C 64.03, H 4.84, N 4.48, Found: C 64.16, H 4.55, N 3.81%.

General procedure of the synthesis of CNC-pincer complexes: An oven dried Schlenk tube with magnetic stirring bar was charged with ligand precursor (1 equiv.), bidentate metal precursor (1 equiv.), and NaI (0.149 g, 1mmol) in ethylene glycol (10 ml), the resulted mixture was refluxed under N_2 atmosphere for 4 h. On completion of the reaction, cooled it to room temperature, add aqueous solution of KPF_6 (0.184 g, 1 mmol, 10 ml water), then stirred for 2 min at room temperature. A desired complex was precipitated out, filtered the precipitate, washed with H_2O and dried under vacuum.

Synthesis of 3a: This complex was prepared by general procedure, using 2,6-Bis[3-(methyl)imidazoliumpyridine dibromide (0.100 g, 0.25 mmol) and **1a** (0.096 g, 0.25 mmol) to give the desired complex as a yellowish orange solid. The X-ray quality crystals of **3a** were obtained by slow diffusion of diethyl ether in methanol solution at 4 ˚C. Yield = 0.129 g (67%). M.P. 278 ºC. HRMS for $[M\text{-}PF_6]^+$ ($C_{22}H_{22}N_8RuI$) in CH_3CN: Calculated: 627.0056, Found: 627.0079. ^1H NMR (400 MHz, DMSO, Component **a**:**b** ratio 45:55) δ 10.27 (d, *J* = 5.7 Hz, 1H) (**a**), 9.81 (d, *J* = 5.8 Hz, 1H) (**b**), 8.51 (d, *J* = 1.9 Hz, 2H), 8.45 – 8.40 (m, 4H),

8.31 – 8.24 (m, 3H), 8.16 (dd, *J* = 8.0, 3.3 Hz, 2H), 8.13 – 8.11 (m, 2H), 8.11 – 8.09 (m, 1H) 7.96 (d, *J* = 8.1 Hz, 2H), 7.68 – 7.62 (m, 1H), 7.58 (d, *J* = 1.9 Hz, 2H), 7.46 (t, *J* = 6.3 Hz, 1H), 7.42 (d, *J* = 1.9 Hz, 2H), 7.31 (d, *J* = 1.9 Hz, 1H), 7.13 (d, *J* = 2.0 Hz, 1H), 3.12 (s, 6H) (**b**), 2.99 (s, 6H) (**a**), 2.55 (s, 3H) (**a**), 2.51 (s, 3H) (**b**). ^{13}C NMR (126 MHz, DMSO) δ 193.30, 188.90, 187.04, 183.34, 156.06, 153.56, 153.38, 152.49, 152.13, 151.93, 141.56, 139.00, 137.76, 136.92, 125.98, 125.37, 124.55, 124.23, 122.49, 121.24, 118.67, 117.59, 117.09, 116.40, 115.26, 112.72, 107.95, 105.46, 35.84, 35.31, 34.17, 33.73. ^{31}P NMR (202 MHz, DMSO) δ -144.20.

Synthesis of 3b: This complex was prepared by general procedure, using 2,6-Bis[3-(methyl)imidazoliumpyridine dibromide (0.100 g, 0.25 mmol) and **1b** (0.103 g, 0.25 mmol) to give the desired complex as a brown-yellow solid. Yield = 0.130 g (65%). M.P. 218 ºC. HRMS for $[M\text{-}PF_6]^+$ ($C_{24}H_{26}N_8RuI$) in CH_3CN: Calculated: 655.0369, Found: 655.0365. ^{1}H NMR (500 MHz, DMSO, Component **a**:**b** ratio 33:67) δ 10.29 (d, *J* = 5.7 Hz, 1H) (**a**), 9.81 (d, *J* = 5.8 Hz, 1H) (**b**), 8.57 (d, *J* = 2.0 Hz, 1H), 8.54 (d, *J* = 1.8 Hz, 2H), 8.48 (d, *J* = 8.2 Hz, 1H), 8.46 – 8.44 (m, 1H), 8.43 (d, *J* = 1.8 Hz, 1H), 8.40 (d, *J* = 2.1 Hz, 1H), 8.29 (d, *J* = 4.1 Hz, 2H), 8.16 (d, *J* = 8.2 Hz, 3H), 7.98 (d, *J* = 8.2 Hz, 1H), 7.93 (d, *J* = 8.2 Hz, 1H), 7.66 (d, *J* = 5.1 Hz, 1H), 7.63 (d, *J* = 2.1 Hz, 1H), 7.61 (d, *J* = 1.9 Hz, 2H), 7.44 (d, *J* = 2.0 Hz, 1H), 7.40 (d, *J* = 2.2 Hz, 1H), 3.13 (s, 6H) (**b**), 2.99 (s, 3H) (**a**), 2.59 (m, 1H) (**a**), 2.19 (m, 1H) (**b**), 0.76 (d, *J* = 6.7 Hz, 6H) (**b**), 0.70 (d, *J* = 6.7 Hz, 3H) (**a**). ^{13}C NMR (126 MHz, DMSO) δ 196.65, 193.68, 187.17, 181.28, 156.22, 153.63, 153.52, 152.44, 152.11, 151.60, 141.95, 139.09, 138.07, 136.99, 125.71, 124.46, 124.40, 122.49, 120.08, 118.48, 118.02, 117.59, 116.98, 112.75, 111.21, 107.76, 105.90, 105.22, 49.88, 49.04, 37.73, 35.87, 35.34, 30.70, 22.02, 21.69. ^{31}P NMR (202 MHz, DMSO) δ -144.19.

Synthesis of 3c: This complex was prepared by general procedure, using 2,6-Bis[3-(methyl)imidazoliumpyridine dibromide (0.036 g, 0.11 mmol) and **1c** (0.050 g, 0.11 mmol) to give the desired complex as a green-yellow solid. Yield = 0.042 g (46%). M.P. 254 ºC. HRMS for $[M\text{-}PF_6]^+$ ($C_{26}H_{24}N_8RuI$) in CH_3CN: Calculated - 677.0213, Found - 677.0242. ^{1}H NMR (500 MHz, DMSO, Component **a**:**b** ratio 57:43) δ 10.44 (d, *J* = 5.5 Hz, 1H) (**a**), 9.90 (d, *J* = 5.7 Hz, 1H) (**b**), 8.70 (d, *J* = 8.5 Hz, 1H), 8.57 (d, *J* = 8.6 Hz, 1H), 8.53 (d, *J* = 2.0 Hz, 2H), 8.49 (d, *J* = 8.2 Hz, 1H), 8.46 (d, *J* = 2.0 Hz, 2H), 8.43 (d, *J* = 2.1 Hz, 1H), 8.37 (d, *J* = 2.7 Hz, 1H), 8.23 (d, *J* = 8.2 Hz, 1H), 8.17 (d, *J* = 8.2 Hz, 2H), 8.02 (d, *J* = 8.2 Hz, 2H), 7.93 (d, *J* = 8.2 Hz, 1H), 7.71 (t, *J* = 6.6 Hz, 1H), 7.60 (d, *J* = 2.1 Hz, 2H), 7.58 (d, *J* = 2.0 Hz, 2H), 7.55 (d, *J* = 1.9 Hz, 1H), 7.54 – 7.50 (m, 1H), 7.47 (d, *J* = 1.9 Hz, 1H), 7.43 (d, *J* = 2.0 Hz, 2H), 7.38 (d, *J* = 4.3 Hz, 2H), 7.37 (d, *J* = 4.3 Hz, 1H), 3.12 (s, 5H) (**b**), 3.00 (s, 6H) (**a**), 2.73 (s, 2H) (**b**), 2.72 (s, 3H) (**a**). ^{13}C NMR (126 MHz, DMSO) δ 196.66, 191.85, 189.18, 186.19, 156.62, 153.39, 152.88, 152.64, 151.61, 151.01, 143.02, 141.90, 139.25, 138.53, 137.88, 136.08, 130.19, 130.02, 125.54, 124.52, 122.11, 120.95, 118.75, 117.59, 117.24, 117.06, 113.57, 113.40, 112.63, 112.13, 111.43, 111.01, 109.81, 108.21, 106.06, 105.93, 37.73, 35.90, 35.41, 35.00, 30.80, 30.44. ^{31}P NMR (202 MHz, DMSO) δ -144.20.

Conflicts of interest

There are no conflicts of interest to declare.

Acknowledgements

This research was supported by the Science and Engineering Research Board, Government of India (EMR/2016/004076). RKS acknowledges CSIR, New Delhi and both NS acknowledge IIT Indore for research fellowship. SIC, IIT Indore and DST-FIST 500MHz NMR Facility, Department of Chemistry, IIT Indore, are acknowledged for characterisation data. All authors gratefully acknowledge the reviewers of a previous submission for their comments which helped shape this paper in its current form.

References

1 T. Ishizuka, H. Sugimoto, S. Itoh and T. Kojima, *Coord. Chem. Rev.*, 2022, **466**, 214536.
2 A. Udvardy, F. Joó and Á. Kathó, *Coord. Chem. Rev.*, 2021, **438**, 213871.
3 T. Ikariya, K. Murata and R. Noyori, *Org. Biomol. Chem.*, 2006, **4**, 393–406.
4 M. R. Axet and K. Philippot, *Chem. Rev.*, 2020, **120**, 1085–1145.
5 E. Peris, *Chem. Rev.*, 2018, **118**, 9988–10031.
6 O. Schuster, L. Yang, H. G. Raubenheimer and M. Albrecht, *Chem. Rev.*, 2009, **109**, 3445–3478.
7 J. DePasquale, M. Kumar, M. Zeller and E. T. Papish, *Organometallics*, 2013, **32**, 966–979.
8 A. Ghaderian, S. Kazim, M. Khaja Nazeeruddin and S. Ahmad, *Coord. Chem. Rev.*, 2022, **450**, 214256.
9 P. Nareddy, F. Jordan and M. Szostak, *ACS Catal.*, 2017, **7**, 5721–5745.
10 J. Pospech, I. Fleischer, R. Franke, S. Buchholz and M. Beller, *Angew. Chem. Int. Ed.*, 2013, **52**, 2852–2872.
11 C. K. Prier, D. A. Rankic and D. W. C. MacMillan, *Chem. Rev.*, 2013, **113**, 5322–5363.
12 A. Kajetanowicz and K. Grela, *Angew. Chem. Int. Ed.*, 2021, **60**, 13738–13756.
13 Q. Zhao, G. Meng, S. P. Nolan and M. Szostak, *Chem. Rev.*, 2020, **120**, 1981–2048.
14 Z.-Q. Wang, X.-S. Tang, Z.-Q. Yang, B.-Y. Yu, H.-J. Wang, W. Sang, Y. Yuan, C. Chen and F. Verpoort, *Chem. Commun.*, 2019, **55**, 8591–8594.
15 E. M. Poland and C. C. Ho, *Appl Organomet Chem*, **n/a**, e6746.
16 S. Thota, D. A. Rodrigues, D. C. Crans and E. J. Barreiro, *J. Med. Chem.*, 2018, **61**, 5805–5821.
17 C. Mari, V. Pierroz, S. Ferrari and G. Gasser, *Chem. Sci.*, 2015, **6**, 2660–2686.
18 X. Ma, S. G. Guillet, M. Peng, K. Van Hecke and S. P. Nolan, *Dalton Trans.*, 2021, **50**, 3959–3965.
19 B. Alcaide, P. Almendros and A. Luna, *Chem. Rev.*, 2009, **109**, 3817–3858.
20 C. W. Bielawski, D. Benitez and R. H. Grubbs, *Science*, 2002, **297**, 2041–2044.
21 S. Aghazada, I. Zimmermann, V. Scutelnic and M. K. Nazeeruddin, *Organometallics*, 2017, **36**, 2397–2403.
22 F. Chen, F. Xiao, W. Zhang, C. Lin and Y. Wu, *ACS Appl. Mater. Interfaces*, 2018, **10**, 26964–26971.
23 L. Mauri, A. Colombo, C. Dragonetti, D. Roberto and F. Fagnani, *Molecules*, 2021, **26**, 7638.

24 A. Del Zotto, W. Baratta, M. Ballico, E. Herdtweck and P. Rigo, *Organometallics*, 2007, **26**, 5636–5642.
25 X. Ma, S. G. Guillet, Y. Liu, C. S. J. Cazin and S. P. Nolan, *Dalton Trans.*, 2021, **50**, 13012–13019.
26 26 T. Lübbering, P. D. Dutschke, A. Hepp and F. E. Hahn, *Organometallics*, 2021, **40**, 3775–3784.
27 Í. Ferrer, J. Rich, X. Fontrodona, M. Rodríguez and I. Romero, *Dalton Trans.*, 2013, **42**, 13461.
28 R. G. Belli, Y. Wu, H. Ji, A. Joshi, L. P. E. Yunker, J. S. McIndoe and L. Rosenberg, *Inorg. Chem.*, 2019, **58**, 747–755.
29 A. K. Singh, B. G. Levine, R. J. Staples and A. L. Odom, *Chem. Commun.*, 2013, **49**, 10799.
30 X. He, Y. Li, H. Fu, X. Zheng, H. Chen, R. Li and X. Yu, *Organometallics*, 2019, **38**, 1750–1760.
31 P. Hermosilla, P. García-Orduña, F. J. Lahoz, V. Polo and M. A. Casado, *Organometallics*, 2021, acs.organomet.1c00453.
32 R. S. Ghadwal, *Dalton Trans.*, 2016, **45**, 16081–16095.
33 E. A. Martynova, N. V. Tzouras, G. Pisanò, C. S. J. Cazin and S. P. Nolan, *Chem. Commun.*, 2021, **57**, 3836–3856.
34 N. V. Tzouras, F. Nahra, L. Falivene, L. Cavallo, M. Saab, K. Van Hecke, A. Collado, C. J. Collett, A. D. Smith, C. S. J. Cazin and S. P. Nolan, *Chem. Eur. J.*, 2020, **26**, 4515–4519.
35 A. Collado, J. Bohnenberger, M. Oliva-Madrid, P. Nun, D. B. Cordes, A. M. Z. Slawin and S. P. Nolan, *Eur. J. Inorg. Chem.*, 2016, **2016**, 4111–4122.
36 K. I. Goldberg and A. S. Goldman, Eds., *Activation and Functionalization of C—H Bonds*, American Chemical Society, Washington, DC, 2004, vol. 885.
37 E. Peris, in *N-Heterocyclic Carbenes in Transition Metal Catalysis*, ed. F. Glorius, Springer Berlin Heidelberg, 2007, vol. 21, pp. 83–116.
38 D. Yadav, S. Misra, D. Kumar, S. Singh and A. K. Singh, *Appl Organomet Chem*, DOI:10.1002/aoc.6287.
39 D. Yadav, R. K. Singh, S. Misra and A. K. Singh, *Appl Organomet Chem*, 2022, **36**, e6756.
40 D. Yadav, R. K. Singh, S. Singh, P. M. Shirage and A. K. Singh, *J Organomet Chem*, 2021, **953**, 122061.
41 41 S. Hitzel, C. Färber, C. Bruhn and U. Siemeling, *Organometallics*, 2014, **33**, 425–428.
42 P. L. Arnold and A. C. Scarisbrick, *Organometallics*, 2004, **23**, 2519–2521.
43 Y. Shimoyama, T. Ishizuka, H. Kotani, Y. Shiota, K. Yoshizawa, K. Mieda, T. Ogura, T. Okajima, S. Nozawa and T. Kojima, *Angew. Chem.*, 2016, **128**, 14247–14251.
44 F. Chen, G.-F. Wang, Y.-Z. Li, X.-T. Chen and Z.-L. Xue, *Inorg. Chem. Commun.*, 2012, **21**, 88–91.
45 D. F. Evans, *J. Chem. Soc.*, 1959, 2003–2005.
46 Y. Cheng, J.-F. Sun, H.-L. Yang, H.-J. Xu, Y.-Z. Li, X.-T. Chen and Z.-L. Xue, *Organometallics*, 2009, **28**, 819–823.
47 G. F. Caramori, A. O. Ortolan, R. L. T. Parreira and E. H. da Silva, *J Organomet Chem*, 2015, **799–800**, 54–60.
48 L. Vaquer, P. Miró, X. Sala, F. Bozoglian, E. Masllorens, J. Benet-Buchholz, X. Fontrodona, T. Parella, I. Romero, A. Roglans, M. Rodríguez, C. Bo and A. Llobet, *ChemPlusChem*, 2013, **78**, 235–243.
49 H.-W. Tseng, R. Zong, J. T. Muckerman and R. Thummel, *Inorg. Chem.*, 2008, **47**, 11763–11773.
50 G. M. Sheldrick, *Acta Crystallogr A Found Crystallogr*, 2008, **64**, 112–122.
51 L. J. Farrugia, *J Appl Crystallogr*, 2012, **45**, 849–854.
52 L. J. Farrugia, *J Appl Crystallogr*, 1997, **30**, 565–565.
53 F. Neese, F. Wennmohs, U. Becker and C. Riplinger, *J. Chem. Phys.*, 2020, **152**, 224108.
54 F. Neese, *WIREs Computational Molecular Science*, **n/a**, e1606.
55 Y. Zhao and D. G. Truhlar, *J. Chem. Phys.*, 2006, **125**, 194101.
56 A. D. Kulkarni and D. G. Truhlar, *J. Chem. Theory Comput.*, 2011, **7**, 2325–2332.
57 A. V. Marenich, C. J. Cramer and D. G. Truhlar, *J. Phys. Chem. B*, 2009, **113**, 6378–6396.
58 H. Kruse and S. Grimme, *J. Chem. Phys.*, 2012, **136**, 154101.
59 C. Adamo and V. Barone, *J. Chem. Phys.*, 1999, **110**, 6158–6170.
60 A. Hellweg, C. Hättig, S. Höfener and W. Klopper, *Theor Chem Acc*, 2007, **117**, 587–597.
61 E. Caldeweyher, J.-M. Mewes, S. Ehlert and S. Grimme, *Phys. Chem. Chem. Phys.*, 2020, **22**, 8499–8512.
62 G. J. Barbante, P. S. Francis, C. F. Hogan, P. R. Kheradmand, D. J. D. Wilson and P. J. Barnard, *Inorg. Chem.*, 2013, **52**, 7448–7459.
63 C. J. Stanton, C. W. Machan, J. E. Vandezande, T. Jin, G. F. Majetich, H. F. Schaefer, C. P. Kubiak, G. Li and J. Agarwal, *Inorg. Chem.*, 2016, **55**, 3136–3144.
64 M. Nirmala and P. Viswanathamurthi, *J Chem Sci*, 2016, **128**, 1725–1735.